

# Microfluidic Interfacial Tensiometry\*

S. D. Hudson,<sup>1</sup> J. T. Cabral,<sup>2</sup> W. Zhang,<sup>1</sup> J. A. Pathak,<sup>1</sup> and Kathryn L. Beers<sup>1</sup>

<sup>1</sup>National Institute of Standards and Technology, Polymers Division, Gaithersburg, MD 20899

<sup>2</sup>Imperial College London, Chemical Engineering, London, UK

## INTRODUCTION

Immiscible fluids find diverse applications, yet their interfacial tension  $\sigma$  remains a fundamental property that governs their performance. Therefore, accurate and efficient methods to measure interfacial tension facilitate development and refinement of fluid formulations. Microfluidic technology offers a new high-throughput platform for such measurements. In our approach, drops are produced and their dynamics in an extensional flow gradient are analyzed in real-time, and applicability to a broad range of interfacial tension is demonstrated.<sup>1</sup>

## METHOD

**Experimental.** The microchannel tensiometer was fabricated by conventional rapid prototyping methods (Figure 1). The master was made by contact photolithography using 365 nm uv exposure and SU-8-2025 or 2075 resists (Microchem<sup>2</sup>) spin coated on a plasma-cleaned silicon wafer. A poly(dimethylsiloxane) (PDMS; Sylgard 184, Dow Corning<sup>2</sup>) replica was then made from the master and cored for inputs and outputs. The patterned PDMS surface and a clean glass slide were oxidized for 35 s with a 40 W oxygen plasma (Anatech-SP100<sup>2</sup>) and brought in contact within seconds thereafter, irreversibly sealing the device, which was finally connected to syringes with Teflon capillary tubing, which fits tightly in the cored inlets and outlets.

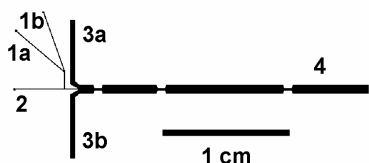


**Figure 1.** Schematic flow channel diagram of the microfluidic tensiometer.

The microfluidic tensiometer is mounted on an inverted optical microscope (Olympus IX71<sup>2</sup>). Computer-controlled syringe pumps (e.g., New Era NE-1200<sup>2</sup>) drive the flow inputs. The pumps are connected in series and then, via RS-232, onto a desktop computer running LabVIEW 7.0.<sup>2</sup>

During operation, fluids 1 a and b are injected into fluid stream 2 and emerge as drops after intersection with streams 3 a and b (Figure 1). The constrictions in channel 4 accelerate and therefore stretch the drops. Fluid drops are imaged with bright field optical microscopy using 4X or 10X objective lenses having numerical apertures  $NA = 0.13$  and  $0.30$ , respectively. Images are captured with a monochromatic CCD camera with  $240 \times 1000$  pixel resolution, 8-bit depth and 100 frames per second (Adimec 1000 M<sup>2</sup>). Depending on the objective used, image magnification ranges from  $0.74$  to  $1.85 \mu\text{m}/\text{pixel}$  and was calibrated using a diffraction grating. The image integration time should be sufficiently small to generate sharp images of drops, such that their motion during acquisition is less than a full pixel and therefore causes no blurring. Typical integration times range from  $20$  to  $100 \mu\text{s}$ , depending on drop velocity.

**Analysis.** The viscosities of the fluids ( $h_d$ ,  $h_c$ ) are the only input variables in the analysis and should be known accurately, because this uncertainty propagates directly to  $s$ . For improved accuracy, we compute

the Arrhenius temperature dependence of the viscosity from reference data and interpolate  $h$  at the relevant temperature, which is recorded during the tensiometric measurements.

Under small deformations, the dynamics of drop stretching and retraction are well understood,<sup>3-5</sup> and described by the following:

$$t \frac{dD}{dt} = D_{\text{steady}} - D = \frac{5}{2\dot{\epsilon} + 3} t \dot{\epsilon} - D \quad (1)$$

where  $D$  is the scalar deformation parameter defined by the difference of the major and minor radii of a spheroidal drop divided by their sum. The relaxation time  $\tau$  depends on drop size, fluid viscosities and interfacial tension.

When drops enter the observation window preceding the channel constriction their velocity is constant ( $\dot{\epsilon} = 0$ ) and they are therefore spherical, and the equilibrium radius of a drop is determined. Since each image contains several drops, an indexing procedure is implemented to identify *each* drop as it moves through the observation window in a sequence of time frames. As the fluid accelerates through the channel constriction, the drop extends slightly.  $D$  is computed from the drop's moments of inertia in every frame. The position of the drop  $x$  is also recorded and assigned a time stamp, from which transit time  $t(x)$  and velocity are calculated. The procedure is repeated for all drops in each image. The system collects and plots over 100 data points per second.

At prescribed time intervals (a few seconds), compiled data for  $D$  and  $t(x)$  are fit to polynomials (order ranging from 4 to 7) to compute terms in equation 1. Plotting this equation for relatively small  $D < 0.1$ , produces a linear correlation, whose slope yields  $s$ .

## RESULTS and DISCUSSION

Our microfluidic tensiometry has been validated against conventional pendant drop tensiometry and other measurements reported in the literature with an array of model immiscible systems, involving water, air, silicone and mineral oils, ethylene glycol and glycerol (Figure 4).<sup>1</sup> A rather wide range of accessible tensions has been demonstrated, ranging from ( $2.5$  to  $60$ )  $\text{mN}/\text{m}$  so far, with broader range of applicability expected. The most significant technological limitation concerns the maximum achievable ratio  $\sigma/\eta_c$ , which is determined largely by camera features such as the maximum frame rate and minimum exposure time. Device geometry and drop size also play significant roles.

Mixtures of ethylene glycol and water suspended in silicone oil have also been characterized. The ratio of ethylene glycol and water are adjusted simply through their rates of injection. The measured interfacial tension approximates a geometric average rule of mixtures, as expected.

## ACKNOWLEDGEMENTS

The support of ICI / National Starch, Procter and Gamble, and the NIST Materials Science and Engineering Laboratories Director's Reserve is gratefully acknowledged. This work was carried out in the NIST Combinatorial Methods Center ([www.nist.gov/combi](http://www.nist.gov/combi)).

## REFERENCES

1. Hudson, S. D.; Cabral, J. T.; Goodrum Jr., W. J.; Beers, K. L.; Amis, E. J. *Applied Physics Letters* **2005**, *submitted*.
2. Certain commercial materials and equipment are identified in this paper in order to adequately specify the experimental procedure. In no case does such identification imply recommendation or endorsement by the National Institute of Standards and Technology, nor does it imply that these are necessarily the best available for the purpose.
3. Taylor, G. I. *Proc.Roy.Soc.(London)* **1934**, *A146*, 501.
4. Taylor, G. I. *Proc.Roy.Soc.(London)* **1932**, *A138*, 41.
5. Rallison, J. M. *Ann.Rev.Fluid Mech.* **1984**, *16*, 45.

\* Official contribution of the National Institute of Standards and Technology; not subject to copyright in the United States.